JOURNAL OF NEUROPHYSIOLOGY
Vol. 68, No. 2, August 1992. *Printed in U.S.A.*

Motor Cortical Activity During Drawing Movements: Single-Unit Activity During Sinusoid Tracing

ANDREW B. SCHWARTZ
Division of Neurobiology, Barrow Neurological Institute, Phoenix, Arizona 85013

SUMMARY AND CONCLUSIONS

1. This study examines the neuronal activity of motor cortical cells associated with the production of arm trajectories during drawing movements. Three monkeys were trained to perform two tasks. The first task ("center→out" task) required the animal to move its arm in different directions from a center start position to one of eight targets spaced at equal angular intervals and equal distances from the origin. Movements to each target were in a constant direction, and the average rate of neuronal discharge with movements to different targets varied in a characteristic pattern. A cosine tuning function was used to map each cell's discharge rate to the direction of arm movement. This function spanned all movement directions, with a peak firing rate in the cell's preferred direction.

2. The second task ("tracing" task) required the animal to trace curved figures consisting of sine waves of different spatial frequencies and amplitudes. Both the speed and direction changed continuously throughout these movements. The cosine tuning function derived from the center→out task was used to model the activity of the cell during the tracing of sinusoids in the second task. Sinusoidal data were divided into 20-ms bins; instantaneous direction, speed, and discharge rate were analyzed bin by bin. This provided a way to compare directly the tuning parameters during a task with constant direction to a task where the direction varied continuously.

3. Movement direction as it changed during the tracing task was an important factor in the discharge pattern of cells that had discharge patterns that could be represented by the cosine tuning function.

4. The modulation of discharge rate during figure tracing depended on both the cell's preferred direction and the orientation of the figure. The activity of cells with preferred directions perpendicular to the axis of the sinusoidal figure was most modulated, whereas the activity of those cells with preferred directions aligned to the figure's axis was least modulated.

5. The cells with modulated activity tended to have firing rates that differed from the predicted cosine tuning function during the sinusoidal movements for those portions of the trajectory where the movement direction was in the cell's preferred direction.

6. Finger speed during figure tracing varied inversely with path curvature with the same relation that has been found during human drawing. To assess the relation of instantaneous speed to discharge rate, the component of the discharge pattern related to direction was subtracted from the total discharge. A comparison between speed and this residual discharge showed that these two parameters were best related when the movement direction was near the cell's preferred direction.

7. Movement direction was consistently represented in the activity of single cells throughout the time course of the movement, whereas speed, which accounted for less of the variance in the spike train than direction, was best represented when the direction of movement was near each cell's preferred direction. These results show that kinematic parameters of movement (direction and speed) related to the arm's trajectory are represented in the discharge pattern of motor cortical cells. These kinematic parameters vary continuously during drawing. Because these parameters can specify the complete trajectory of the arm, the information encoded in the activity of these neurons may adequately describe the shape of the drawn figure.

INTRODUCTION

The trajectory of the arm is an important element in the control of volitional reaching and pointing. This study was designed to test the idea that arm trajectory is explicitly represented in the activity of motor cortical cells as the arm moves. Experimental evidence suggests that the arm's trajectory is controlled continuously during volitional movement. The shape of the arm's trajectory is preserved in deafferented animals even when perturbed (Bizzi et al. 1984). The spatial variability of the trajectory is small with repeated reaches to the same target and becomes even smaller with practice (Georgopoulos et al. 1981). The arm path is not affected by speed (Soechting and Lacquaniti 1981) or weights applied to the arm (Lacquaniti et al. 1982). Direct evidence of the central representation of trajectory comes from neuronal studies (Georgopoulos et al. 1988). With the use of a technique to visualize the ongoing population response of an ensemble of motor cortical cells, the encoded image of the trajectory was found to precede and predict point-to-point movements through three-dimensional (3D) space. These studies characterized issues related to straight movement, but it is not clear that these findings are valid for the large class of movements resulting in curved trajectories. Trajectory is obviously important in drawing tasks. The path of the hand is the relevant aspect of the behavior that corresponds to the shape of the drawn figure. Many of the properties of drawing movements (Lacquaniti et al. 1982; Soechting et al. 1986; Soechting and Terzuolo 1987a,b; Viviani and Stucchi 1989; Viviani and Terzuolo 1982) elucidated by psychophysical experiments suggest that the control of these movements is organized to facilitate the transformation of an internal representation of the shape to be drawn into a selected set of joint angles and torques used to implement the movement.

The trajectory may be decomposed temporally into a series of vectors. Each vector is specified by a direction and a magnitude; these components define tangential velocity. If the vectors are defined at constant temporal intervals, the magnitude of each vector is speed. Although it is useful to study speed and direction separately, in certain movements such as drawing they may not be independent. As the spa-

tial rate of directional change (curvature) increases, the angular velocity decreases (Lacquaniti et al. 1983; Viviani and Terzuolo 1982). The present study examines both movement direction and movement speed as it is continuously represented in the activity of motor cortical neurons during the tracing of sinusoidal figures. This approach was taken in an attempt to show whether and how curved arm trajectories may be encoded in the motor cortex.

METHODS

Behavioral paradigm

Rhesus monkeys (*Macaca mulatta*, male 2–4 kg, 3 animals) were seated in a primate chair with one arm completely free to move. The chair was positioned in front of a capacitive touch-sensitive computer monitor (22.5 × 17.5 cm) so that a point midway between the monkey's shoulders was aligned to the center of the screen. The screen was approximately in the frontal plane (slanted at a 15° angle to the vertical). Each monkey was trained to draw with its index finger on the surface of the screen. Initially the animals were conditioned to perform the center→out task, which is similar to a task described previously in the horizontal plane (Georgopoulos et al. 1981). A target circle (1- or 1.1-cm radius) appeared in the middle of the screen. The animal placed its finger in this circle and held it there for a variable period of time (300–500 ms) until one of eight targets spaced at equal angular intervals 6 cm from the center appeared. The monkey then moved its finger on the screen surface to the peripheral target, holding it there (200–400 ms) until a reward was given. If the animal failed to acquire the target within 500 ms or lifted its finger from the screen, the trial was aborted. Five repetitions of the eight targets were presented in a randomized block design (Cochran and Cox 1957). The entire behavioral paradigm as well as the data acquisition was controlled by a laboratory microcomputer.

On completion of the center→out task, the monkey performed the sinusoid task. This task was designed so that the monkeys would make a natural, smooth drawing movement within approximately a 1-cm band around the presented figure. A target circle (10- to 11-mm radius) would appear at the edge of the screen. The animal placed its finger in the circle, which served as the starting location (hold A) for the sine wave that appeared on the screen 200–500 ms later. Five different sinusoidal shapes were used ranging from 3 to 12 cm in height. The horizontal extent of each sinusoid was ~15.5 cm, and the number of cycles presented varied from one to four. Each figure was centered vertically on the screen. As the figure appeared, the target circle jumped a small increment along the sine wave, and the animal moved its finger along the screen surface to the target. The beginning of the movement was considered to be the instant the finger moved out of the boundary of the original hold A circle (this resulted in some minor temporal inaccuracy as the finger had a non-zero speed at this point). As soon as the finger reached the target, the circle jumped to the next location on the sine wave. In this way the circle always stayed just ahead of the animal's finger, and the animal was free to move at its own pace. The distance the circle jumped along the trajectory was determined empirically so that the drawing rate of the graphics interface could erase and redraw the circle rapidly enough to stay ahead of the animal's movement. This distance was between 1.5 and 2 cm at equal intervals along the figure. This sequence continued until the finger crossed the limit of the last target circle at the end of the figure, at which point the animal was immediately rewarded. Typically, the animals learned to make smooth and graceful movements after 3 mo of training. Although the wrist and fingers were free to move, the animals invariably adopted a strategy where they traced with their index finger extended and the rest of the fingers flexed. The finger and wrist angles varied little during the movement so that the proximal joints were primarily responsible for the displacement of the finger tip along the figure. Each figure was traced from left to right then in the opposite direction and presented five times in a randomized block design. Each sinusoidal shape traced in a particular direction was considered a different experimental class.

Neural recordings

After the animals were trained, a 19-mm-diam stainless steel cylinder was surgically implanted through the skull over the motor cortex. On the following recording days, the head was fixed mechanically and a Chubbuck microdrive placed over the chamber, sealing it hydraulically. The electrode was placed at precise locations in the chamber with the use of an x-y stage. These locations were noted and used as a record of the penetration positions. Typically, one transdural penetration using a glass-coated platinum-iridium electrode was carried out daily. Recording sessions were limited to 4–6 h after which the microdrive was removed, the chamber sealed, and the animal returned to its cage. Activity from cells in a given hemisphere (contralateral to the performing arm) was recorded for ~30 days. Unitary activity was identified by the use of standard extracellular techniques (Georgopoulos et al. 1982; Schwartz et al. 1988). In addition to recording a cell's activity during the task, its activity was monitored as the animal's arm was manipulated and when the monkey reached for raisins in different locations. This examination was undertaken to determine whether the activity was related to passive and or active shoulder movement and to ensure that it was not related exclusively to finger, wrist, or other spurious movements such as licking or chewing; such cells were not included in the data base. Small lesions were occasionally placed electrolytically (2–3 μA for 3–5 s) at the end of a penetration. These were used to mark the location and extent of the electrode track.

Data collection and analysis

The occurrence of each spike was recorded relative to the start of the trial with a 1-ms resolution and buffered with the use of an interface (CED 1401) attached to the laboratory computer (Compaq 386). The computer controlled the touchscreen display and recorded the position of the animal's finger every 20 ms. The behavioral information, finger positions, and spike data were written to disk between trials.

CENTER→OUT TASK. The analysis of direction-dependent discharge during this task has been described previously (Georgopoulos et al. 1982). The average discharge rate of an isolated cell was calculated for movements to each of the eight targets in the different directions (θ). This rate was calculated from fractional intervals during the epoch from the onset of the peripheral target to its acquisition. For the purpose of visualization, these data were aligned to the instant the finger exited the center target. Because this target was 2.2 cm diam, the finger was often moving at a substantial speed at the exit point. This had no bearing on the analysis, because the reaction and movement time comprised a single epoch over which the data were averaged.

A multiple regression was used to find the constants b_0, b_1, and b_2 for the tuning equation

$$D = b_0 + b_1 \sin\theta + b_2 \cos\theta \qquad (1)$$

where D is the discharge rate, b_0 is the grand mean of rates found in movements to the eight targets, b_1 is the y component of maximum discharge in the preferred direction, and b_2 is the x component of maximum discharge. This function can also be written in linear form

$$D = b_0 + k \cos(\theta - \theta_0) \quad (2)$$

$$k = \sqrt{b_1^2 + b_2^2}$$

$$\theta_0 = \tan^{-1}\left(\frac{b_1}{b_2}\right)$$

According to this equation the maximum discharge occurs with movements in the preferred direction, θ_0

$$\theta_0 = \theta, \quad D = b_0 + \sqrt{b_1^2 + b_2^2}$$

A cell was considered "tuned" if 70% of the variance in discharge rate was explained by the regression ($r^2 \geq 0.7$; $P < 0.001$).

TRACING TASK. The discharge rates of tuned cells recorded during the sinusoid task were compared with the rates predicted by the use of the tuning functions calculated from the center→out task. The spike discharge rates were calculated throughout the task at 20-ms intervals (see DATA REDUCTION). The predicted discharge rate was based only on the relation between movement direction and discharge rate. This prediction was used to characterize the directional component of the total discharge pattern found in the tracing task. The direction the finger moved in each bin was calculated and used to find the predicted discharge rate from the center→out tuning function as follows. Tuning constants b_0, b_1, and b_2 were derived from the results of the center→out task. The movement direction, θ, was calculated for each bin of the sinusoidal trajectory averaged over the repeated trials of the same class for a particular cell. *Equation 2* was then used to find the predicted rate of discharge for that bin. Note that the discharge rate expressed in *Eq. 2* for the center→out task is the average rate over the epoch that includes the reaction and movement times for the entire task. The rate used in the prediction for the tracing task assumed that this expression represented the instantaneous rate in a 20-ms bin. The prediction for a given cell and class was compared with the actual pattern with the use of cross correlation. Results from this analysis were plotted as lag (the interval between a point in the actual rate profile and a point in the predicted rate profile that occurred τ ms later) versus the correlation coefficient. The peak correlation coefficient of this analysis shows how well the cosine tuning function (*Eq. 1*) derived from the center→out task represents the actual rates of discharge in the tracing task. High correlation suggests that the simple representation of straight direction in the center→out task takes place continuously during the curved movements.

To illustrate the influence of different preferred directions on the predicted discharge profile, a series of simulations was performed. Simulated patterns of discharge in the tracing task were calculated for a set of hypothetical cells with different preferred directions. Movement direction as it changed over the sinusoidal trajectories was used in *Eq. 2*. For each simulation, b_0 had a value of 30, and k had a value of 40 spikes/s. The only variable that changed between simulations was θ_0, the preferred direction. Depth of modulation in discharge rate was defined in simulations by the difference between maximum and minimum rates in the trial. The depth of modulation in the actual spike data was found in the same way, except the data were smoothed (double-sided, 5-point exponential) first.

DATA REDUCTION. Typically, each of the 10 sinusoidal patterns (5 shapes × 2 directions) were drawn 5 times as they were presented in a random block during the experiment pertaining to a particular cell. Spike data were reduced by averaging over the five repeated trials of each sinusoidal class (pattern). The averaging took place in the following way. The mean trial duration was found for each class. This mean duration was divided by 20 ms to give an average number of bins n. Each trial was divided into n bins by adjusting the binwidth appropriately. Fractional intervals were calculated in each bin and converted into a rate by dividing by the binwidth. The counts in each bin were summed across trials and divided by the number of trials for that class. Speed data were normalized to n bins by the use of a spline function on the displacement data. X- and y-coordinates were normalized separately, then differentiated to give incremental distance in each dimension. These were either combined to give speed (speed = $\sqrt{\Delta x^2 + \Delta y^2}$), or the arctangent used to give direction. This procedure made it possible to compare the various parameters in a bin-by-bin manner.

RESULTS

Simulations

One aspect of this study is to determine whether the cosine function describing the firing rate of a cortical neuron as it relates to direction for point-to-point movements is also valid for drawing movements where the direction of movement changes continuously. The profile of the discharge rate during sinusoid drawing is dependent on the cell's preferred direction and can be illustrated with simulations. Simulations representing the neuronal responses of cells with different preferred directions were calculated with *Eq. 2*. With the use of this tuning formula, it was possible to generate a discharge rate profile for the given sinusoidal trajectories by calculating the tangent angle at equal spatial intervals through the trajectory. The tangent angle, representing instantaneous direction, is then used in *Eq. 2* as θ. In the same equation, b_0 was chosen as 40 spikes/s and k as 30 spikes/s. The discharge profiles for two simulated sinusoids drawn in two different directions are shown in Fig. 1

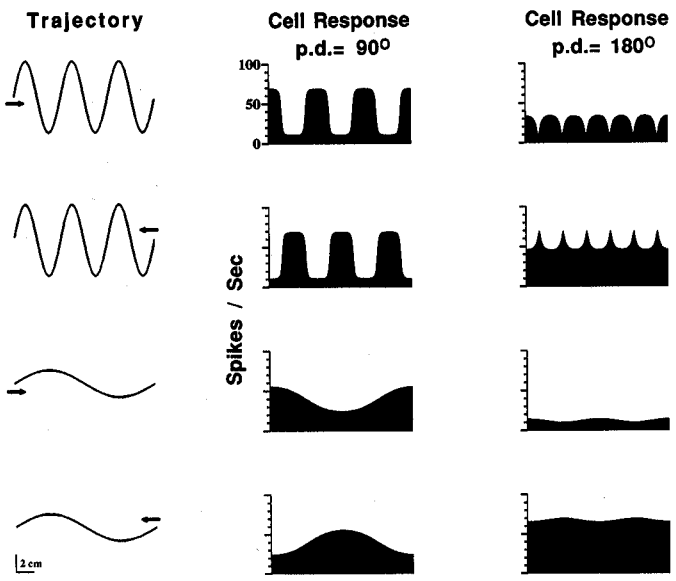

FIG. 1. Simulated responses. Sinusoids representing trajectories are shown in the *left column*. Each pair is the same figure drawn in opposite directions as indicated by the arrows. Both axes have units of centimeters, and the calibration is shown in the *bottom left corner*. The *top 2 traces* were simulated to approximate classes 2 and 7, the *bottom 2 traces* approximate classes 4 and 9. The *middle column* shows the calculated response of a "cell" with a preferred direction of 90° (upward). The *right column* shows the corresponding response of a cell with a horizontal preferred direction of 180° (leftward). Responses were calculated according to the tuning formula: $D = b_0 + k \cos(\theta - \theta_0)$ where b_0 was 40 and k was 30 spikes/s. θ was the instantaneous direction calculated as the tangent of the sinusoid, and θ_0 was the preferred direction.

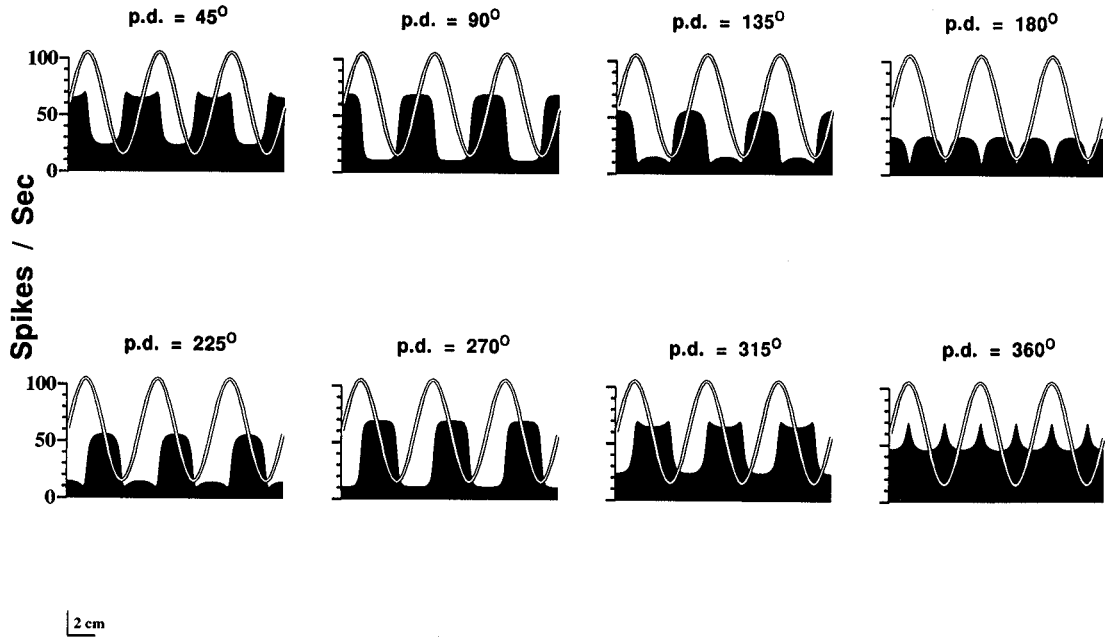

FIG. 2. Simulated responses. This figure shows the simulated responses of a series of cells with different preferred directions during the drawing of the same sinusoid. The sinusoidal trajectory (outline) is superimposed on the simulated response (shaded histogram). The same tuning formula used in Fig. 1 is used here.

for a preferred direction, θ_0, of 90 (vertical) and 180° (horizontal). Movement direction in the simulated sinusoid with the high spatial frequency is primarily in the vertical direction, nearly 90°, once per cycle. These upward movements are followed by movements in almost the opposite direction (~270°). Because the preferred direction is 90°, the cell will fire at a near maximum rate ($b_0 + k = 70$ spikes/s) for this sinusoid during the upward portion of the trajectory and at a minimal rate ($b_0 - k = 10$ spikes/s) for the downward portion. When the preferred direction is changed to 180°, the rate profile is much different. In this case the movement is in the preferred direction only at the peak of each cycle, although the movement direction is never farther than 90° from the preferred direction. This leads to a profile that is much less modulated than that for vertical preferred directions. The relation between preferred direction and depth of modulation could also be seen when lower amplitude sinusoids with lower spatial frequencies were simulated. In this trajectory the direction components are primarily horizontal. Although the depth of modulation in the simulated responses of the cell with the vertical preferred direction is reduced compared with the higher frequency trajectory, it is still much greater than the simulated response of the cell with the horizontal preferred direction. This "horizontal cell" fired at almost a constant rate that was near maximal in the simulation of the leftward drawing and near its minimal rate for the rightward movement.

The high-frequency trajectory and the same values for b_0 and k were used to simulate the responses of a series of cells with different preferred directions in Fig. 2. The rate profiles changed in an orderly fashion, and the depth of modulation in these responses varied smoothly with changes in preferred direction. The depth of modulation was greatest with the vertical preferred directions (90 and 270°) and minimal with the horizontal directions (180 and 360°).

Recording sites

Sites of electrode penetrations ($n = 111$) in which directionally tuned cells related to proximal arm movement were encountered are shown in Fig. 3. Single-unit activity

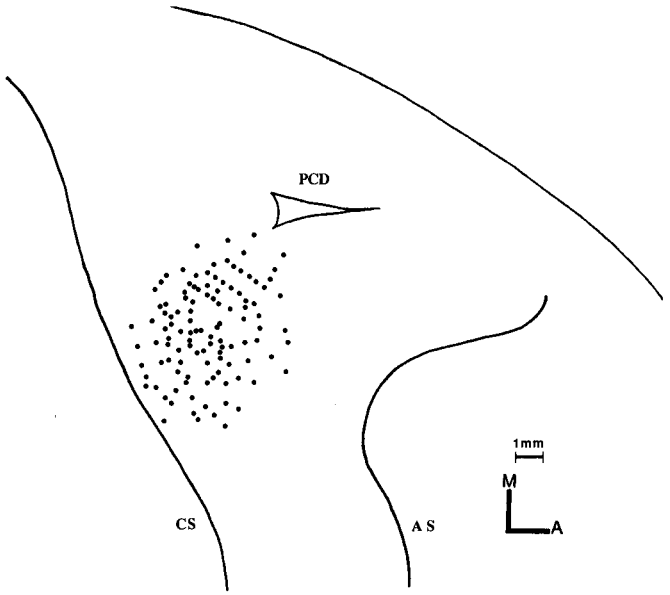

FIG. 3. Recording sites. This schematic shows the electrode penetration sites for the cell responses recorded in this study. The electrode locations from 5 hemispheres (2 left and 3 right) are superimposed on this drawing of a right hemisphere. CS, central sulcus; AS, arcuate sulcus; PCD, precentral dimple; M, medial, A, anterior.

of 357 tuned cells recorded in 5 hemispheres of 3 animals was used in this study.

Center→out task

Activity during the center→out task of the cell shown in Fig. 4*A* was represented by a tuning function with a peak firing rate for movements made 283° (preferred direction) from the horizontal (Fig. 4*B*). Average discharge rate for each movement was calculated for the epoch that began with appearance of the peripheral target and ended when this target was acquired. Cell activity tended to be greatest for downward movements and minimal for upward movements. The function is unimodal, spans the directional domain, and is identical to the function previously described for movement tasks in the horizontal plane (Georgopoulos et al. 1982).

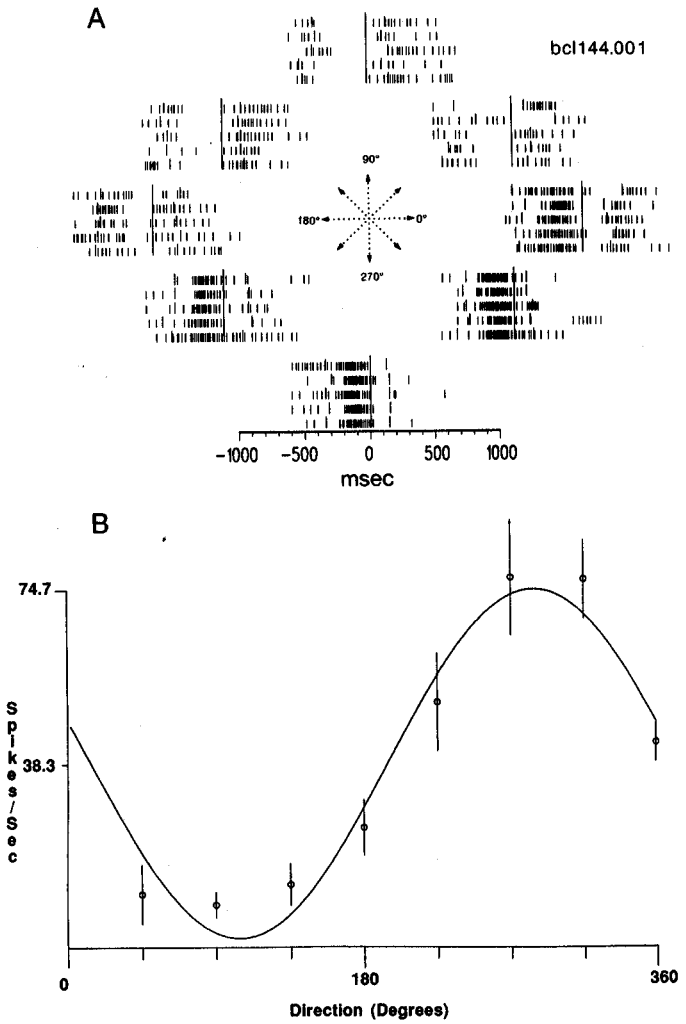

FIG. 4. Discharge patterns during the center→out task. *A*: rasters are arranged schematically at each target location around the center start position. Each raster is aligned to the exit from the center start position ($T = 0$). The 1st long tick mark of each trial is the target onset time, the 2nd is the time of movement onset, and the 3rd is the time of target acquisition. *B*: the cosine tuning function was derived from the average rate of discharge between target onset and target acquisition for each movement (open circles). The vertical line through each circle is the standard deviation of that average rate. A cosine tuning function was fit to these data: $D = b_0 + k \cos(\theta - \theta_0)$, $b_0 = 37.9$, $k = 36.1$, (the units are spikes/s), $r^2 = 0.95$.

The displacement data collected during the center→out task for all cells used in this study were averaged and speed profiles calculated as described in METHODS. The profiles for the same experimental epochs described above are shown in Fig. 5. Each profile is aligned to the instant the finger crossed the center target boundary. The portion of the profile before this has a duration equal to the average (mean of 5 repetitions to that target) epoch length between the onset of the peripheral target and the exit from the center target, whereas the remaining portion has a duration equal to the average time it took to reach the peripheral target after leaving the center target. This figure shows that the finger was moving rapidly as it left the center target and when it arrived at the peripheral target. The speed profiles for the different movements were nearly identical as were the peak speeds (30.3 ± 1.1 cm/s) to each target. This shows that different speeds were not a factor in determining the directional tuning parameters derived from the center→out task.

Sinusoid task

Average finger trajectories of all the sinusoidal movements in this study are displayed in Fig. 6. The number beside each trace is the experimental class corresponding to the sinusoid presented. Classes 1–5 were drawn from left to right across the screen. Matching classes (6–10) were drawn in the opposite direction. These finger trajectories were always within 1 or 1.1 cm of the figure presented on the screen. Although the horizontal extent of each sinusoid was 17 cm, the horizontal length of the recorded movement trajectory will be smaller because the movement epoch was considered to begin after the finger moved from the target hold zone, which had a 1- or 1.1-cm radius. The movement was considered finished when the finger entered the terminal target zone at the end of the figure, which also had the same radius.

Whereas direction was constant in each movement of the center→out task and the data from each movement was averaged over the entire movement epoch, the speed, direction, and discharge rate varied continuously as each sinusoid was drawn. This made it necessary to use analytic techniques that could compare these parameters throughout the task. An example of the intramovement relation between movement speed and direction is shown in Fig. 7, where these parameters are compared bin by bin. Movement speed is approximately proportional to the radius of curvature in figure drawing (Lacquaniti et al. 1983; Viviani and Terzuolo 1982). The radius of curvature in a sinusoid is largest in the middle of each wave and smallest at each peak. Thus the speed will be greatest in the middle, vertical region of the sinusoid and smallest at the peaks, where the movement is horizontal. The speed and movement direction for each 20-ms bin of every sinusoidal class in the data base was plotted in the scatter plot. The speed increased in the vertical portions (90 and 270°) of the sinusoid. Notice that the peak speeds in the center→out (30 cm/s) task are comparable with the range of speeds encountered in the sinusoid task.

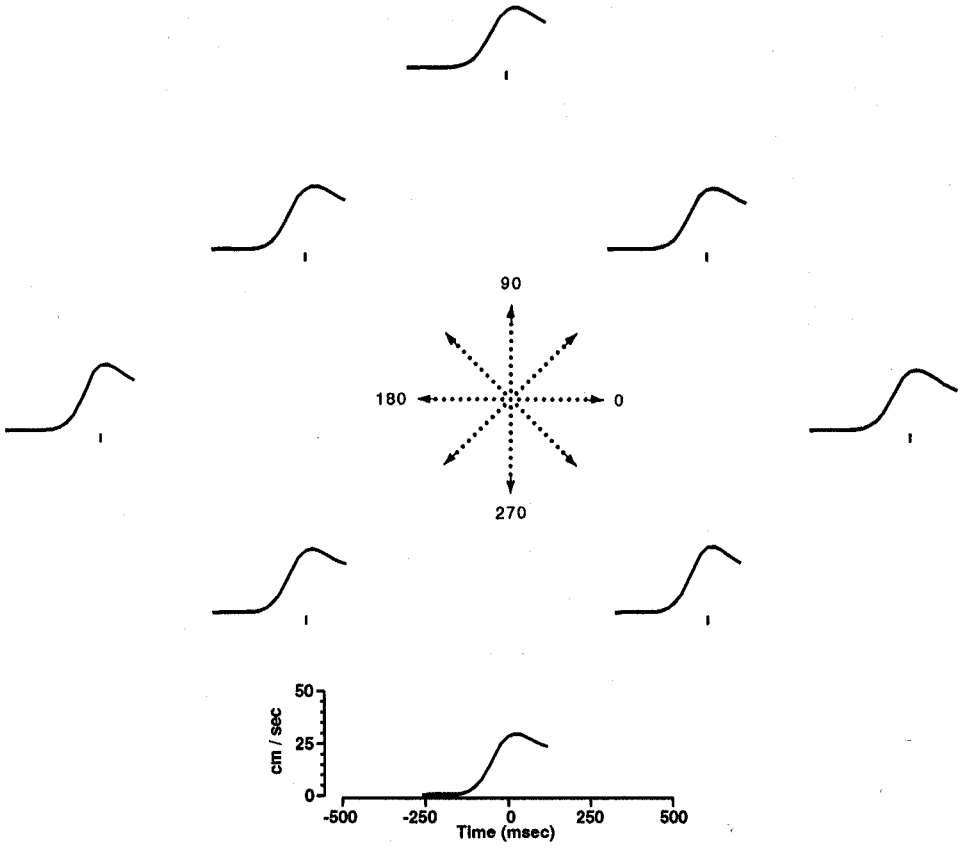

FIG. 5. Speed profiles during the center→out task. This figure is arranged in the same manner as Fig. 4*A*. Profiles were normalized and averaged across the data base (356 cells). The portion of the profile before the alignment point began at stimulus onset and was normalized separately from the latter portion. The entire profile has a duration equal to the mean duration for that direction. Each profile is aligned to the exit from the center target. At this point the finger was moving near its maximum speed. The profile shape and maximal speeds were nearly identical for movements in the different directions.

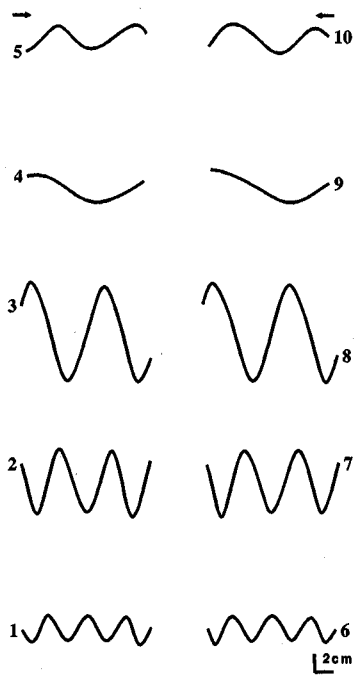

FIG. 6. Finger trajectories. These trajectories are averages of all the drawings made by the animals in this study. Trajectories for individual trials were normalized to 100 bins before averaging. There were 5 sinusoids each traced from left to right then in the opposite direction for a total of 10 classes. Class numbers are shown at the starting location of each trace. Arrows show the direction the sinusoid was traced; those in the *left column* were traced rightward, those in the *right column* were traced leftward. Both axes have units of centimeters.

Discharge pattern during sinusoid task

RELATION OF DISCHARGE RATE TO MOVEMENT DIRECTION. This cell's activity (same unit as shown in Fig. 4) during the sinusoid task is represented in Fig. 8. The numbering scheme is the same as that of Fig. 6 with each raster aligned to the exit of the finger from the initial hold target. The rasters show that this cell was consistently well modulated throughout the figure. Displacement data superimposed on these rasters show that the cell began to fire at the top of the sinusoids, before the finger moved downward. The spike data are represented as smoothed histograms (shaded) in Fig. 9. Superimposed on these histograms is the predicted discharge rate. The predicted pattern is derived from the cosine tuning function by the use of the same methodology as that in the simulations except that the predicted pattern used directions from the actual finger trajectory (see METHODS). The predicted pattern was calculated at 20-ms intervals, whereas the simulated profiles were calculated at regular spatial intervals. Because the movement speed was not constant throughout the movement, the simulated (i.e., constant speed) and predicted rate profiles will be slightly different in shape. Essentially, the predicted pattern shows how closely the actual discharge pattern follows the relation described in *Eq. 2*. The prediction is similar to the actual rate, although there is a consistent undershoot and a lag of the prediction. The shape of the predicted pattern results from the way that direction varies in the sinusoidal pattern (i.e., direction is relatively constant for vertical portions of the figure). The correspondence between predicted and ac-

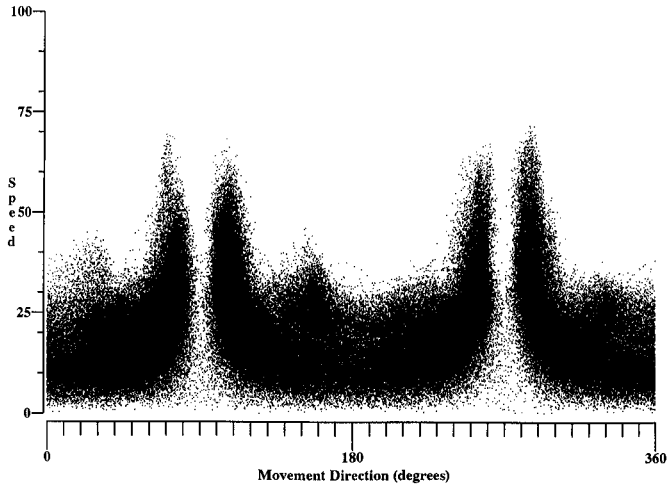

FIG. 7. Scatter plot of direction vs. speed. The instantaneous movement direction and speed were calculated for each 20-ms bin through all the sinusoid experiments in the data base. The speed tended to be greatest in the vertical portions of the sinusoid, which were also the straightest and tended to be smallest at the curved, horizontal peaks. A wide range of speeds was generated in this task. Gaps in the plot at 90 and 270° are from the lack of movement in these directions. The animals did not make movements along the absolute vertical. The ordinate is in cm/s.

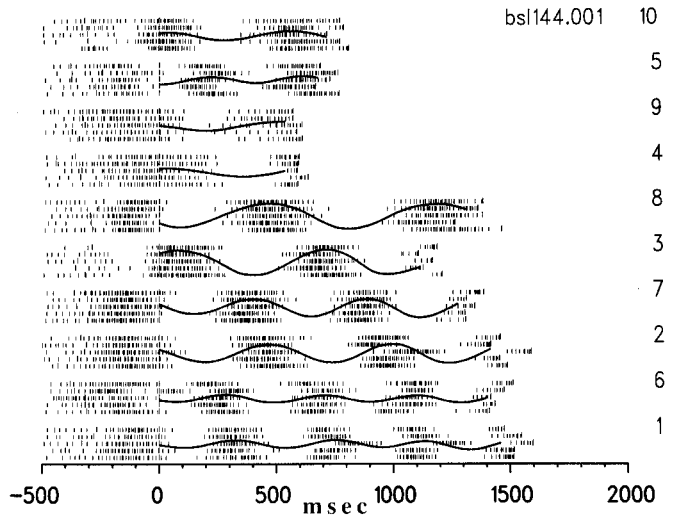

FIG. 8. Rasters derived from the tracing task. Rasters are arranged by class. Class numbers correspond to those of Fig. 6. Each raster is aligned to the exit from the initial target. The 1st long tick mark in each record is the time that the sinusoid pattern was presented, the 2nd long tick mark is the time of movement onset, and the 3rd is when the task was completed. The sinusoidal line through each raster is the average y-position of the finger at that time in the trial. The cell firing increased each time the finger moved downward and stopped firing for upward movements.

tual rates can be assessed by the use of cross correlation (Fig. 10). For example, the peak correlation of class 1 sine waves, moving from left to right, occurs at a lag of 120 ms with a correlation coefficient of 0.88. Construction of the predicted pattern of discharge is essentially a transformation of movement direction to discharge rate. The validity of this operation is represented by the peak correlation coefficient. With the use of this argument, the lag (120 ms) between the signals is the interval between the direction encoded by the neuron and movement of the arm in that direction. Because the correlation was high, the lag between the traces must be consistent throughout the trial. The lag between the 10 different classes was fairly consistent (138 ± 21 ms).

The residuals found by shifting the prediction by the corresponding lag and subtracting it from the actual pattern are shown in Fig. 11. The residuals for this cell are cyclical and are largest at the peaks of firing rate where the predic-

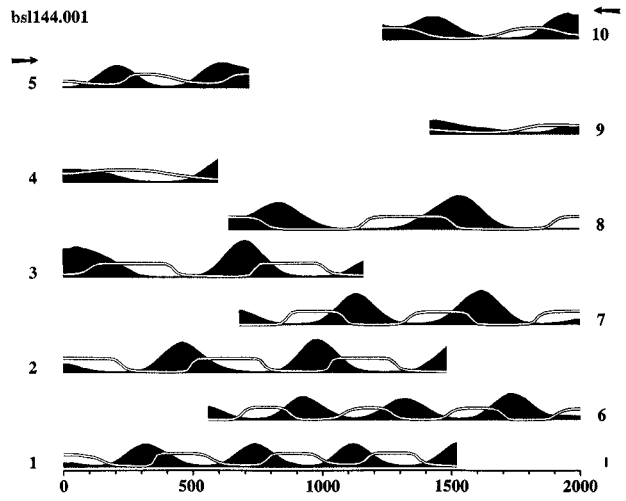

FIG. 9. Actual and predicted rates. Each pattern is arranged by class. Discharge patterns of rightward movements begin at $T = 0$; those of leftward movements begin at $T = 2{,}000$. Units along the abscissa are milliseconds. The shaded pattern is a histogram (normalized to the average movement duration for that class) of the actual firing rates. The solid, heavy trace is the predicted rate of discharge. The vertical calibration bar represents 50 spikes/s. The predicted rate lags the actual rate and has flattened maxima. The prediction consistently underestimates the actual peak firing rates.

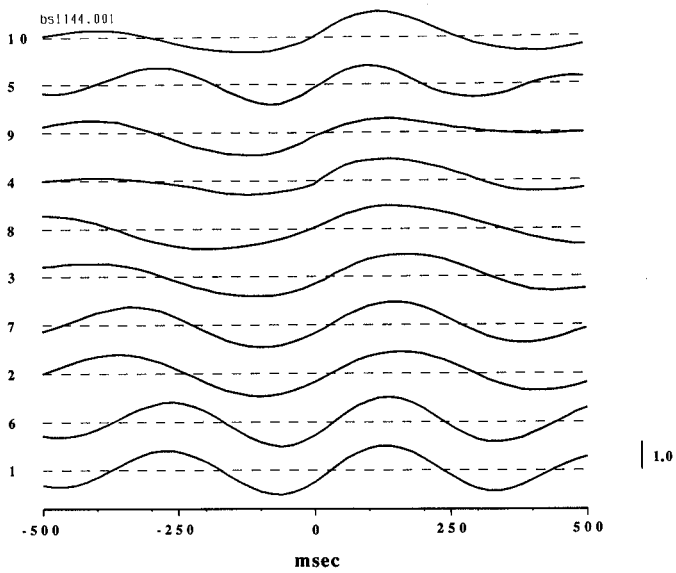

FIG. 10. Cross correlograms between predicted and actual discharge rates. Correlograms (same cell as Figs. 4, 8, and 9) are arranged by class. The abscissa is lag in milliseconds. The calibration bar is $r = 1.0$. The 1st positive peak after $\tau = 0$ occurs consistently across classes ($\tau = 138 \pm 21$ ms).

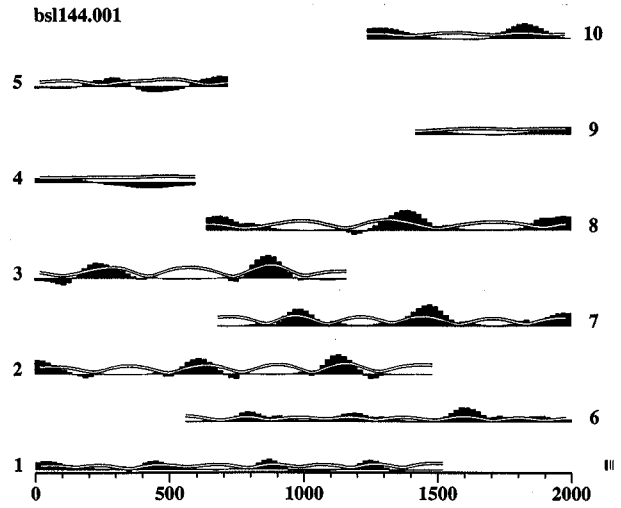

FIG. 11. Residuals between actual and predicted discharge rates. This figure is based on the data of Fig. 9 and also has the same layout (the abscissa is in ms). The predicted rate was shifted relative to that of the actual by the lags determined from the cross correlation. The predicted rate was then subtracted from the actual rate. The outline superimposed on the histogram is speed. The left calibration bar is 50 spikes/s, the right is 50 cm/s.

tion consistently undershoots the actual rate. Superimposed on the residual pattern of Fig. 11 is the speed of the finger. The magnitude of the residual rate corresponds to the alternating peaks of finger speed. The correspondence is present in the cycles where the finger is moving in the cell's preferred direction. This will be addressed in detail in a later section.

The correspondence between predicted and actual discharge patterns for a cell with a horizontal preferred direction is shown in Fig. 12. This cell's preferred direction was 354°, and it tended to fire fastest for movements made to the right. As expected from the simulations, the discharge profile of this cell was not consistently modulated. This cell fired at a high rate when the figures were drawn from left to right (classes 1–5) and tended not to fire in the opposite direction classes (6–10). This is especially evident for classes 4, 5, 9, and 10, where the low-frequency sinusoids of small amplitude were drawn. The cross correlations calculated on individual classes suggest that the correspondence between the predicted and actual rates is poor and not consistent (Fig. 13). This is partially due to the low depth of modulation (small variance) within each class and the use of the cross-correlation function on data restricted to individual classes. This issue is addressed in a later section by using a regression that spans different classes (see Fig. 17).

To show that these findings depend on the orientation of the figure, the activity of some of the cells with horizontal preferred directions was recorded while vertically oriented sinusoids were drawn. The response of the same cell shown in Figs. 12 and 13 is displayed in Fig. 14*A* during the drawing of vertical sinusoids. The vertical sinusoid consisted of two cycles with an amplitude of 8 cm. Class 1 was drawn from the bottom to the top of the screen, and class 2 drawn in the opposite direction. The animals were not explicitly trained to perform this task and were presented with these figures occasionally after the horizontal tasks had been completed. As a result, these trajectories were not as smooth and rapid as those from the horizontal trajectories. Nevertheless, compared with the horizontal sinusoids, the depth of modulation increased. This is reflected in the amplitude and shape of the corresponding correlograms in Fig. 14*B*.

The depth of modulation in firing rate for class 3 of each cell in the population is plotted against that cell's preferred direction as shown in Fig. 15. In agreement with the simulations, cells with vertical preferred directions tended to be most modulated, whereas those with horizontal preferred directions were least modulated. Because the correlation

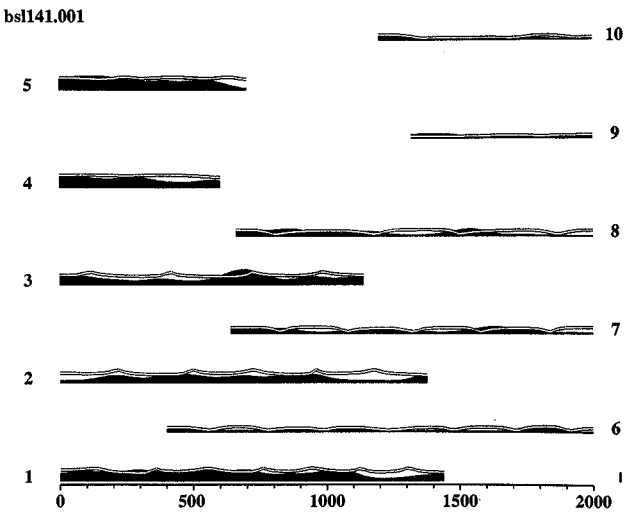

FIG. 12. Predicted and actual discharge rates from a cell with a horizontal preferred direction. This figure has the same format and scale as Fig. 9. This cell's preferred direction was oriented to the right (pd = 354°, b_0 = 37.4 spikes/s, k = 27.9 spikes/s, r^2 = 0.93). The calibration bar has a value of 50 spikes/s. The abscissa is in milliseconds.

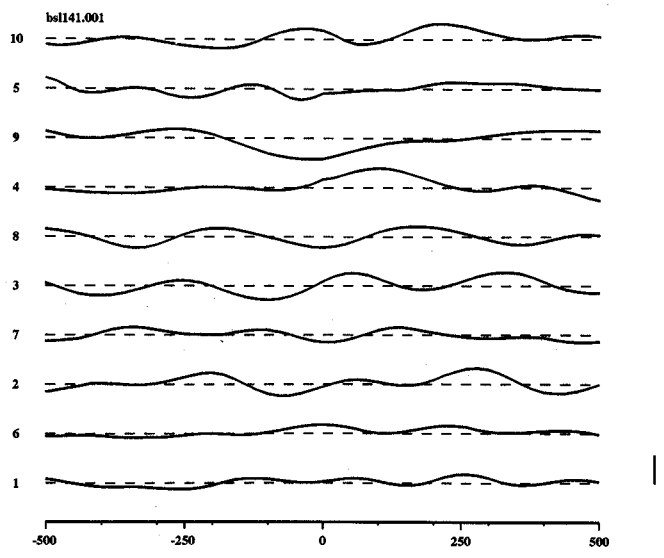

FIG. 13. Cross correlograms of prediction for a cell with a horizontal preferred direction. This figure has the same format as Fig. 10, but displays the cross correlation between the predicted and actual profiles using the data shown in Fig. 12. The correlations were weak and inconsistent. The calibration is r = 1.0, the abscissa is lag time in milliseconds.

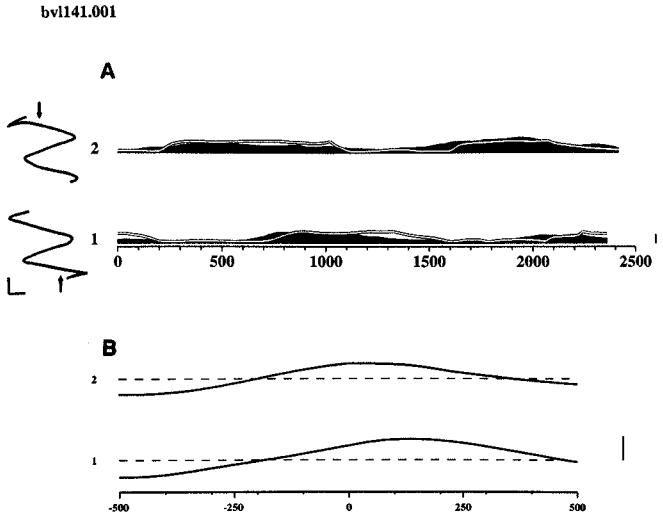

FIG. 14. Response of a horizontal cell when tracing a vertical sinusoid. The trajectory of the finger is shown to the *left* of each histogram in *A*. The sinusoid in class 1 was drawn from bottom to top, for class 2 it was drawn in the opposite direction. These trajectories are the averages from the 110 trials of this task that this monkey performed. Discharge profiles (same scale as Fig. 12) were more modulated than those in Fig. 12, and as shown in *B*, the correlation is also better (the peak correlation coefficient for class 1 was 0.89; for class 2 it was 0.65). The calibration in the *inset* is 2 cm in each direction; in *A* the bar corresponds to 50 imp/s; in *B* it corresponds to $r = 1.0$. The abscissa in *A* is time in milliseconds; in *B* it is lag in milliseconds.

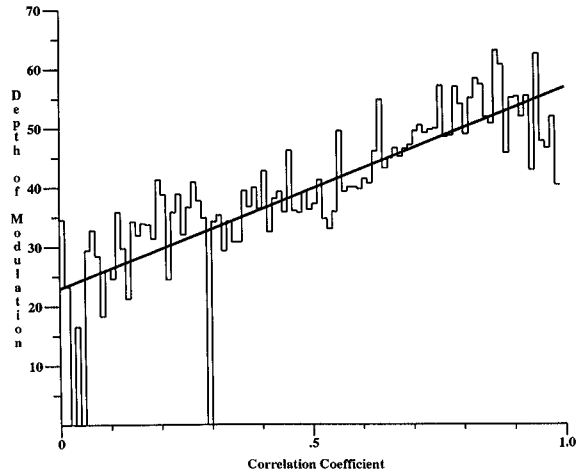

FIG. 16. Depth of modulation vs. peak correlation coefficient. The peak correlation coefficient in the cross correlation between the predicted and actual discharge rates was matched to the depth of modulation for each class of every cell in the data base. A linear regression and correlation were performed on these data ($r = 0.803$, slope = 33.7, 3,358 points). For display purposes, these data were divided into 100 bins along the abscissa and the average taken in each bin. The ordinate has units of spikes/s.

coefficient used to judge the fit of the data to the cosine tuning formula is a measure of how the two signals increase and decrease together, it can be expected that this measure is dependent on the depth of modulation in each signal. This is shown in Fig. 16 where the depth of modulation for each class of sinusoid in every cell was plotted against the corresponding peak correlation coefficient for each class. The relation is direct and linear ($r = 0.803$).

This analysis was organized on a class-by-class basis and is insensitive to the maintained changes in discharge rate observed for the cells with horizontal preferred directions. To assess the directional characteristics of discharge patterns from these cells, a linear regression between discharge rate and direction (shifted by the cross-correlation lag) was performed across classes for each cell. The population of cells was divided into those with horizontal (±45° of both horizontal directions) and those with vertical (±45° of both vertical directions) preferred directions. These overlapping distributions are displayed in Fig. 17 and show that cells with horizontal preferred directions encoded direction as well as those with vertical preferred directions. These findings are in good agreement with the simulations, suggesting that the directional tuning formula accounts for much of the observed pattern of discharge in these motor cortical cells.

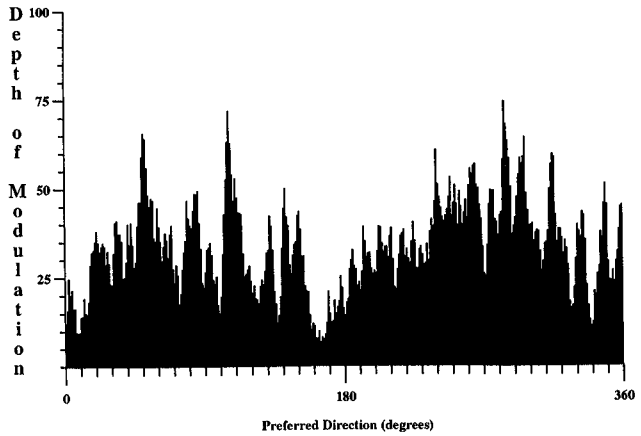

FIG. 15. Depth of modulation in firing rate vs. preferred direction. The depth of modulation (peak-to-peak amplitude) in firing rate was calculated from the averaged and smoothed histograms of each cell's activity for class 3 (357 points). These data were grouped by preferred direction into 1° bins. The average for each bin was calculated, then the average values were smoothed with a double-sided, 5-point exponential function. The depth of modulation tends to be greatest for cells with vertical preferred directions (90 or 270°) and least for those with horizontal preferred directions (0 or 180°). The ordinate has units of spikes/s.

RELATION OF SPEED TO DISCHARGE. Direction is one component of trajectory. If these motor cortex cells encode the trajectory of arm movement, it is necessary for their rates to contain speed information as well. Because direction and speed are considered separately, the component of discharge rate identified as corresponding to direction was removed from the actual discharge profile by shifting the predicted discharge pattern by the correlation lag and subtracting. The resulting residual discharge rate as exemplified in Fig. 9 can be expected to contain information related to parameters other than direction. As shown in this figure, the residuals are greatest when the movement speed is maximal in the cell's preferred direction. This also corresponds to the regions where curvature is small. In this example the correlation between speed and residual rate is conditional on the movement being in the cell's preferred direction. Movement in the opposite direction (upward) does not re-

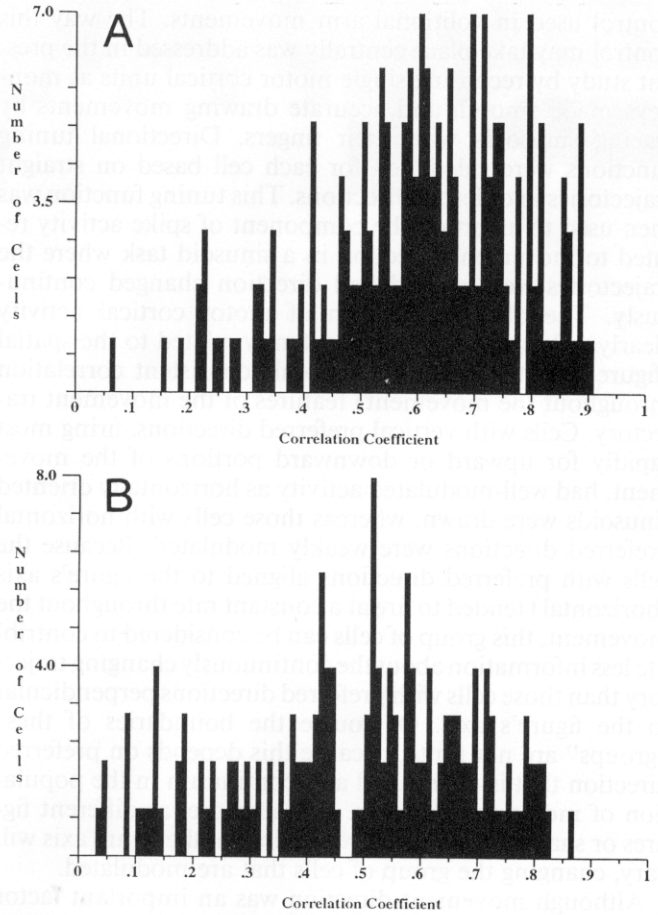

FIG. 17. Directional regression across sinusoid classes. The correlation coefficient from a linear regression between predicted and actual discharge rates using all the data for each recorded cell is plotted in separate histograms for cells with vertical (*A*, 191 cells) and horizontal preferred directions (*B*, 175 cells). Horizontal cells were classified as those with preferred directions ±45° of the horizontal axis, whereas vertical cells had preferred directions within ±45° of the vertical. These distributions overlap, indicating that the responses of the vertical and horizontal cells are equally well described by the directional tuning function.

sult in any substantial residual rate even though it is just as rapid.

A plot comparing residual magnitude to each cell's relative movement direction is shown in Fig. 18. This figure was constructed from a scatter plot in which each point represented the residual discharge rate in a 20-ms bin for a relative movement direction (movement direction − preferred direction) for all the bins in the data base. The residual rate was shifted in time by the lag in the cross correlation for each class. This scatter plot was reduced by dividing the abscissa into 360 bins and calculating the average value for the positive and negative rates separately. This shows that both the positive and negative residuals tend to be greatest for movements in each cell's preferred direction when the cell is firing at its peak rate. Because this shows the results for all cells in the population, and these cells had preferred directions that were distributed in all directions, the residuals tend to be greatest in the cell's preferred direction, independent of the preferred direction or the speed of the finger as it moves in the cell's preferred direction.

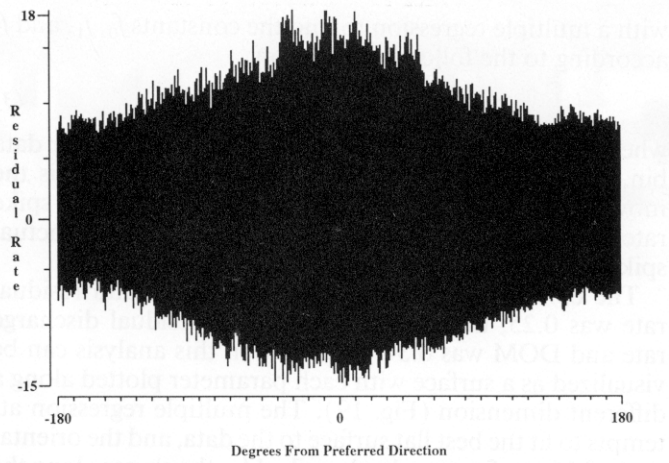

FIG. 18. Residual discharge rate vs. relative direction. A scatter plot was generated with the use of all the bins in the data base. The residual rate (actual − predicted) was calculated for each bin, shifted by the cross-correlation lag and matched to the direction of movement relative to the cell's preferred direction ($\theta - \theta_0$). To better visualize this, the abscissa was divided into 360 bins, and the average residual rate calculated in each bin. This was done separately for the positive and negative residuals. The residuals (spikes/s) were largest for movements in or near each cell's preferred direction.

Because the residuals were greatest near each cell's preferred direction, the data were limited to those bins within ±45° of the preferred direction for each cell. The overall depth of modulation in spike activity and the lag-adjusted speed were then compared with the residual discharge rate

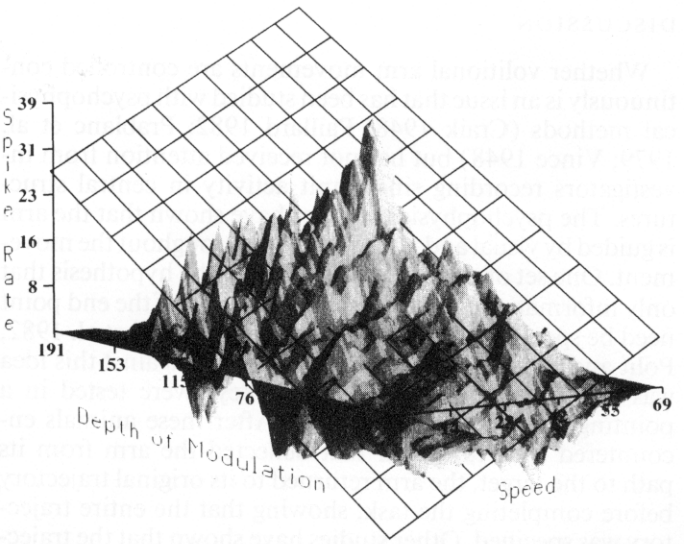

FIG. 19. Comparison of residual rate to depth of modulation and speed (data within 45° of preferred direction). The residual discharge rate (spikes/s) for each bin in the data base was shifted by the appropriate lag and plotted along an axis in a 3 space against the corresponding depth of modulation (spikes/s) in total firing rate and against speed (cm/s), which was plotted along the 3rd axis. These points were reduced by dividing the depth of modulation and speed axes into 100 bins and finding the average residual value in each of the resulting 10,000 volumes. The resulting surface was smoothed. There is a tendency for the residuals to be larger for larger depths of modulation and for higher speeds. A regression surface represented by the superimposed grid shows the plane that best represents the data. It has a slope along the speed axis of 0.38 and a slope along the depth of modulation axis of 0.24.

with a multiple regression to find the constants f_0, f_1, and f_2 according to the following equation

$$d_r = f_0 + f_1 \text{ Speed} + f_2\text{DOM} \quad (3)$$

where d_r is the residual discharge rate for a particular data bin, f_0, f_1, and f_2 are regression coefficients, Speed is the movement speed in the data bin corresponding to the spike rate, and DOM is the depth of modulation for the actual spike rate in the corresponding sinusoidal class.

The correlation coefficient between speed and residual rate was 0.25; the correlation between residual discharge rate and DOM was 0.34. This data in this analysis can be visualized as a surface with each parameter plotted along a different dimension (Fig. 19). The multiple regression attempts to fit the best flat surface to the data, and the orientation of this surface can be described by the slopes along the speed and DOM axes. The slope (f_1) for the speed data was 0.38, which means that the spike rate changed by 26 spikes/s over the range of speeds in the data base. The slope for DOM (f_2) was 0.24, which means that the spike rates associated with this variable had a range of 45 spikes/s. Both of these slopes were significantly different form zero ($P < 0.005$).

The same analysis when calculated on the data for all directions of movement (not restricted to movements near each cell's preferred direction) resulted in a much poorer relation between speed and residual spike rate. In this case the correlation coefficient between the two variables was 0.08, and the slope was 0.085 for a discharge range of only 7 spikes/s.

DISCUSSION

Whether volitional arm movements are controlled continuously is an issue that has been studied with psychophysical methods (Craik 1948; Paillard 1982; Prablanc et al. 1979; Vince 1948) but has not received attention from investigators recording single-unit activity in central structures. The psychophysical studies have shown that the arm is guided by visual and nonvisual cues throughout the movement. One set of experiments addressed the hypothesis that only information about the spatial location of the end point need be specified in pointing movements (Bizzi et al. 1982; Polit and Bizzi 1979). However, evidence against this idea was found when deafferented monkeys were tested in a pointing task (Bizzi et al. 1984). After these animals encountered a perturbation that deflected the arm from its path to the target, the arm returned to its original trajectory before completing the task, showing that the entire trajectory was specified. Other studies have shown that the trajectory is not independent of the target. Rather it is affected by the target's shape, size, and orientation (Pauligan et al. 1990; Soechting 1984). These and other psychophysical studies (Lacquaniti et al. 1983; Soechting 1989; Soechting and Lacquaniti 1981; Soechting and Ross 1984; Soechting and Terzuolo 1987a,b) have begun to uncover the systematic rules used to construct volitional arm movements. The aim of the present study was to describe the relation of motor cortical activity to the movement of the arm as this continuous process evolved throughout a volitional task.

Drawing tasks can be used to elaborate the continuous control used in volitional arm movements. The way this control may take place centrally was addressed in the present study by recording single motor cortical units as monkeys made smooth and accurate drawing movements by tracing sinusoids with their fingers. Directional tuning functions were calculated for each cell based on straight trajectories in different directions. This tuning function was then used to ascertain the component of spike activity related to movement direction in a sinusoid task where the trajectories were curved and direction changed continuously. The observed pattern of motor cortical activity clearly reflected and was consistently related to the spatial (figure orientation) and temporal (consistent correlation throughout the movement) features of the movement trajectory. Cells with vertical preferred directions, firing most rapidly for upward or downward portions of the movement, had well-modulated activity as horizontally oriented sinusoids were drawn, whereas those cells with horizontal preferred directions were weakly modulated. Because the cells with preferred directions aligned to the figure's axis (horizontal) tended to fire at a constant rate throughout the movement, this group of cells can be considered to contribute less information about the continuously changing trajectory than those cells with preferred directions perpendicular to the figure's axis. Of course the boundaries of these "groups" are not finite, because this depends on preferred direction that is distributed as a continuum in the population of motor cortical cells. Furthermore, as different figures or shapes within a figure are drawn, the figure axis will vary, changing the group of cells that are modulated.

Although movement direction was an important factor in the discharge pattern of these cells, other factors seem to be represented in this activity. This was demonstrated by subtracting the activity related to direction (derived from the directional tuning function) from the total activity. Three factors besides movement direction were reflected in this residual activity. The magnitude of the residual rate was greatest when the direction of movement coincided with the cell's preferred direction. This was not simply due to an underestimate of the tuning function, because the residuals were equally likely to be positive as negative (cf. Fig. 18). Because the magnitude of each cell's residual activity was related to its preferred direction and the preferred directions of the cells in this population were evenly distributed over the directional domain, the distribution of residual activity was not biased in any given direction; the magnitudes of residuals are the same for cells with vertical preferred population as for those with horizontal orientations. Within this residual activity, another factor, the speed of movement, was found to be best represented when the movement direction coincided with the cell's preferred direction (i.e., when the residual rate was largest). The last discharge-related factor identified in this study was the depth of modulation in firing rate, which was associated with the orientation of the figure. The depth of modulation tended to be larger for preferred directions perpendicular to the figure axis, and this was reflected in both the directional portion of the spike activity (as illustrated in the simulations) and in the residual activity (cf. Fig. 19). If the magnitude of the residuals reflects the bandwidth of the nondirectional information encoded in the spike train, then well-

modulated neurons have the ability to encode more information.

Information pertaining both to the direction and speed of movement was contained in the discharge patterns of these neurons as demonstrated by the analyses described above. Evidence for encoded trajectory information has also been found in the single-unit activity of areas 4 and 6 (Hocherman and Wise 1991) when monkeys moved their arms through a series of curved movements. These results cannot be taken as proof that the motor areas of cortex are the source of the kinematic control used in these movements, as movement direction has been found to be represented in many areas of the CNS (Caminiti et al. 1990; Crutcher and Alexander 1990; Fortier et al. 1989; Georgopoulos et al. 1982; Kalaska et al. 1983, 1989, 1990). Correlation analyses also cannot distinguish multiple parameters that covary. For instance, in this experiment, speed and curvature were inversely related. The correlation between discharge rate and speed could be expected to be similar to that between discharge rate and the inverse of curvature. Nevertheless, the results of this study show that the available information in the motor cortex pertains to the class of parameters related to movement kinematics, although this does not mean that the activity of these neurons is exclusively related to kinematics.

Recent studies have attempted to categorize specific central structures on the basis of the representation of dynamic or kinematic parameters in the neuronal activity within these areas. Kinematic features of movement, parameters that describe the arm's trajectory, are distinct from dynamics that are the joint torques and segment forces generated in the movement. This issue dates to the original work of Evarts (Evarts 1968), where he first examined motor cortical discharge in behaving monkeys. The important concept in these arguments is that any kinematic representation of the movement ultimately must be described in terms of dynamics (Hollerbach and Flash 1982; Pellionisz and Llnas 1982; Soechting 1989). Subsequent experiments found that dynamic parameters could be represented in motor cortical discharge. The correlation between spike activity and torque was weak (Humphrey 1972) but improved by assuming that each spike produced a pulse of torque that decayed over 250–500 ms. Another study (Schmidt et al. 1975) found that motor cortical activity was unrelated to different loads (spring constants) applied to a manipulandum during the "dynamic" portions of a wrist flexion-extension task, but better related to the activated muscles producing the movement. More recent studies (Crutcher and Alexander 1990; Kalaska et al. 1989; Schmidt et al. 1975; Thach 1978) examining the relation between force and motor cortical activity did not examine the temporal relation of spike activity to force, and these results are difficult to relate to the mechanisms used to generate the movement.

One of these recent studies examined the directional tuning of motor cortical cells as static loads were applied to the arm. Kalaska and his co-workers (Kalaska et al. 1989) using an arm movement task, found that motor cortical cells could be fit with the cosine tuning function and that the primary effect of loads applied to the manipulandum was to shift the cosine function along the ordinate by a constant discharge rate. Because discharge activity averaged over time was compared with a constant load, it was not possible to measure any effects in the temporal pattern of spike activity that may have been related to the torques used to accelerate and decelerate the manipulandum. For example, in the unloaded condition the force used to accelerate the handle would be expected to be equal and opposite to the decelerative force. When such a profile is integrated over time, the result is zero. Any spike activity correlated to these changes in force would go unobserved in this analysis. The authors concluded that there was no force-related change in the movement-related activity of these cells besides the tonic offset due to the static load. In contrast, a short report (Taira et al. 1991) using a technique that compared motor cortical activity and force continuously during an isometric arm task found that firing rate and the net force produced during the task were correlated.

A later study, again using a manipulandum that could be loaded in different directions and monkeys performing the center→out task, found that the static load effect was less prevalent in the activity of area 5 parietal cortex cells (Kalaska et al. 1990). On the basis of differences between the responses in these two areas, a hierarchical scheme was proposed in which movement kinematics encoded in area 5 served as a basis for dynamics coding in area 4. This distinction is difficult because the criteria for dynamics was based on the application of static loads, and those cells with load effects were not shown to have force-related activity during movement (these cells also fit the cosine tuning formula for direction, and their activity may have been related to kinematics). Furthermore, the cell responses showing the best load effects were confined to the central sulcus. More anterior cells in area 4 encoded only movement direction, and their responses were similar to those found in the parietal cortex. Thus it is unclear whether areas 4 and 5 may be differentiated by their neuronal responses to kinematic or dynamic movement parameters.

Another study (Crutcher and Alexander 1990) addressed this hierarchical issue by recording activity in three different structures: motor cortex, supplementary motor cortex, and putamen. Static loads were used in an elbow flexion-extension task. Load and directionally sensitive cells were distributed evenly throughout the three structures, arguing against a hierarchical organization on the basis of this criterion. It was also determined that cells responsive to premovement cues were directionally sensitive, but insensitive to static loads (Alexander and Crutcher 1990). The conclusion drawn was that these brain regions do not code for dynamics during the preparation for movements. However, ~40% of the task-related cells in these three areas did show movement-related load effects, and this activity was similar to the electromyographic (EMG) patterns of the elbow muscles. Although muscle activity may be qualitatively related to muscle force and therefore loosely related to limb dynamics, the transformation between EMG and force may be complex and nonlinear (Agarwal and Gottlieb 1982). If the integrated sum of EMG activity as a function of movement direction resembles the cosine tuning function of motor cortical cells, an argument could be made that the observed EMG activity may be the actual parameter encoded by the motor cortical cells. Indeed, the EMG

activity of many muscles recorded during the two-dimensional center→out task appears to resemble the cosine tuning function (Kalaska et al. 1989), with broad tuning and a single preferred direction. However, this may not be the case when 3D movements are considered (Kettner et al. 1988) or for isometric contractions (Flanders and Soechting, 1990) and arm (Flanders 1991) movements in various planes of free space where the tuning function for specific muscles often has more than one component. Mussa-Ivaldi (1988) argued on theoretical grounds that "equivalent" muscles would have cosine tuning functions. However, his formulation was based on muscle length and assumed that this was linearly related to its torque contribution. This has been shown to be incorrect as arm muscles often are generating active force while lengthening (Soechting 1988) and may be multiarticular or have complex origin-insertion geometry (Wood et al. 1989). For 3D movements the degrees of freedom in the arm allow it to move in nearby directions with different combinations of joint displacements, obligating different patterns of muscle activity for the different movement strategies. This makes it likely that the movement direction-muscle tension relation in the general case of free movements will show several local maxima. In contrast, motor cortical activity in a 3D reaching task can be described with a single cosine function (Schwartz et al. 1988).

The present study applied an approach that emphasized the continuous processing that underlies the generation of volitional movement. The findings here show that the kinematics of arm movement are well represented in the activity of motor cortical cells, although other movement parameters such as those representing dynamics may be simultaneously encoded. A large portion of the pattern of spike activity recorded from these cells was related to movement direction and a smaller (but still significant) portion to movement speed. Although the speed information encoded in the activity of single cells may be imprecise, this activity, when combined to form a population response, predicted movement speed very well (Schwartz and Anderson 1989, 1990). It is possible that a wide range of imprecisely encoded parameters may be more precisely extracted from such ensemble activity. This may be especially important when considering the integrated action of all the motor structures involved in volitional movement. These parameters are reflected in the neuronal activity of multiple structures and may not exist in final form until integrated into the movement itself.

I am grateful to B. Anderson and A. Kakavand for expert technical assistance and patience in training the animals. P. Wettenstein provided electronics support, and B. Kousari assisted in the programming. I would like to thank Drs. J. R. Bloedel, A. P. Georgopoulos, and B. J. Richmond for critical comments on the manuscript.

This study was funded by National Institute of Neurological Disorders and Stroke Grant NS-26375.

Address for reprint requests: Div. of Neurobiology, Barrow Neurological Inst., 350 W. Thomas Rd., Phoenix, AZ 85013.

Received 10 October 1991; accepted in final form 19 March 1992.

REFERENCES

AGARWAL, G. C. AND GOTTLIEB, G. L. Mathematical modeling and simulation of the postural control loop. Part I. *Crit. Rev. Biomed. Eng.* 8: 493–498, 1982.

ALEXANDER, G. E. AND CRUTCHER, M. D. Preparation for movement: neural representations of intended direction in three motor areas of monkey. *J. Neurophysiol.* 64: 133–150, 1990.

BIZZI, E., ACCORNERO, N., CHAPPLE, W., AND HOGAN, N. Arm trajectory formation in monkeys. *Exp. Brain Res.* 46: 139–143, 1982.

BIZZI, E., ACCORNERO, N., CHAPPLE, W., AND HOGAN, N. Posture control and trajectory formation during arm movement. *J. Neurosci.* 4: 2738–2744, 1984.

CAMINITI, R., JOHNSON, P. B., AND URBANO, A. Making arm movements within different parts of space: dynamic aspects in the primate motor cortex. *J. Neurosci.* 10: 2039–2058, 1990.

COCHRAN, W. G. AND COX, G. M. *Experimental Designs.* New York: Wiley, 1957.

CRAIK, K. J. W. Theory of the human in control systems. II. Man as an element in a control system. *Br. J. Psychol.* 38: 142–148, 1948.

CRUTCHER, M. D. AND ALEXANDER, G. E. Movement-related neuronal activity selectively coding either direction or muscle pattern in three motor areas of the monkey. *J. Neurophysiol.* 64: 151–163, 1990.

EVARTS, E. V. Relation of pyramidal tract activity to force exerted during voluntary movement. *J. Neurophysiol.* 31: 14–27, 1968.

FLANDERS, M. Temporal patterns of muscle activation for arm movements in three-dimensional space. *J. Neurosci.* 11: 2680–2693, 1991.

FLANDERS, M. AND SOECHTING, J. F. Arm muscle activation for static forces in three-dimensional space. *J. Neurophysiol.* 65: 1818–1837, 1990.

FORTIER, P. A., KALASKA, J. F., AND SMITH, A. M. Cerebellar neuronal activity related to whole-arm reaching movements in the monkey. *J. Neurophysiol.* 62: 198–211, 1989.

GEORGOPOULOS, A. P., KALASKA, J. F., CAMINITI, R., AND MASSEY, J. T. On the relations between the direction of two-dimensional arm movements and cell discharge in primate motor cortex. *J. Neurosci.* 2: 1527–1537, 1982.

GEORGOPOULOS, A. P., KALASKA, J. F., AND MASSEY, J. T. Spatial trajectories and reaction times of aimed movements: effects of practice, uncertainty and change in target location. *J. Neurophysiol.* 46: 725–743, 1981.

GEORGOPOULOS, A. P., KETTNER, R. E., AND SCHWARTZ, A. B. Primate motor cortex and free arm movements to visual targets in three-dimensional space. II. Coding of the direction of movement by a neuronal population. *J. Neurosci.* 8: 2928–2937, 1988.

HOCHERMAN, S. AND WISE, S. P. Effects of hand movement path on motor cortical activity in awake, behaving rhesus monkeys. *Exp. Brain Res.* 83: 285–302, 1991.

HOLLERBACH, J. M. AND FLASH, T. Dynamic interactions between limb segments during planar arm movement. *Biol. Cybern.* 44: 67–77, 1982.

HUMPHREY, D. R. Relating motor cortex spike trains to measures of motor performance. *Brain Res.* 40: 7–18, 1972.

KALASKA, J. F., CAMINITI, R., AND GEORGOPOULOS, A. P. Cortical mechanisms related to the direction of two-dimensional arm movements: relations in parietal area 5 and comparison with motor cortex. *Exp. Brain Res.* 51: 247–260, 1983.

KALASKA, J. F., COHEN, D. A., PRUD'HOMME, M., AND HYDE, M. L. Parietal area 5 neuronal activity encodes movement kinematics, not movement dynamics. *Exp. Brain Res.* 80: 351–364, 1990.

KALASKA, J. F., COHEN, D. A. D., HYDE, M. L., AND PRUD'HOMME, M. A comparison of movement direction-related versus load direction-related activity in primate motor cortex, using a two-dimensional reaching task. *J. Neurosci.* 9: 2080–2102, 1989.

KETTNER, R. E., SCHWARTZ, A. B., AND GEORGOPOULOS, A. P. Primate motor cortex and free arm movements to visual targets in three-dimensional space. III. Positional gradients and population coding of movement direction from various movement origins. *J. Neurosci.* 8: 2938–2947, 1988.

LACQUANITI, F., SOECHTING, J. F., AND TERZUOLO, C. A. Some factors pertinent to the organization and control of arm movements. *Brain Res.* 252: 394–397, 1982.

LACQUANITI, F., TERZUOLO, C., AND VIVIANI, P. The law relating kinematic and figural aspects of drawing movements. *Acta Psychol.* 54: 115–130, 1983.

MUSSA-IVALDI, F. A. Do neurons in the motor cortex encode movement direction? An alternative hypothesis. *Neurosci. Lett.* 91: 106–111, 1988.

PAILLARD, J. *The Contribution of Peripheral and Central Vision to Visually Guided Reaching.* Cambridge, MA: MIT Press, 1982.

PAULIGAN, Y., MACKENZIE, C., MARTENIUK, R., AND JENNEROD, M. The

coupling of arm and finger movements during prehension. *Exp. Brain Res.* 79: 431–435, 1990.

PELLIONISZ, A. AND LLINAS, R. Space-time representation in the brain. The cerebellum as a predictive space-time metric tensor. *Neuroscience* 7: 2949–2970, 1982.

POLIT, A. AND BIZZI, E. Characteristics of the motor programs underlying arm movements in monkeys. *J. Neurophysiol.* 42: 183–192, 1979.

PRABLANC, C., ECHALIER, J. F., JENNEROD, M., AND KOMILIS, E. Optimal response of eye and hand motor systems in pointing at a visual target. II. Static and dynamic visual cues in the control of hand movement. *Biol. Cybern.* 35: 183–187, 1979.

SCHMIDT, E. M., JOST, R. G., AND DAVID, K. K. Re-examination of force relationship of cortical cell discharge patterns with conditioned wrist movements. *Brain Res.* 83: 213–223, 1975.

SCHWARTZ, A. B. AND ANDERSON, B. J. Motor cortical images of sinusoidal trajectories. *Soc. Neurosci. Abstr.* 15: 788, 1989.

SCHWARTZ, A. B. AND ANDERSON, B. J. Direction and velocity coding in motor cortical cells. *Soc. Neurosci. Abstr.* 16: 423, 1990.

SCHWARTZ, A. B., KETTNER, R. E., AND GEORGOPOULOS, A. P. Primate motor cortex and free arm movements to visual targets in three-dimensional space. I. Relations between single cell discharge and direction of movement. *J. Neurosci.* 8: 2913–2927, 1988.

SOECHTING, J. F. Effect of target size on spatial and temporal characteristics of a pointing movement in man. *Exp. Brain Res.* 54: 121–132, 1984.

SOECHTING, J. F. Effects of load perturbations on EMG activity and trajectories of pointing movements. *Brain Res.* 451: 390–396, 1988.

SOECHTING, J. F. Elements of coordinated arm movements in three-dimensional space. In: *Perspectives on the Coordination of Movement,* edited by S. A. Wallace. Amsterdam: Elsevier/North-Holland, 1989, p. 47–83.

SOECHTING, J. F. AND LACQUANITI, F. Invariant characteristics of a pointing movement in man. *J. Neurosci.* 1: 710–720, 1981.

SOECHTING, J. F., LACQUANITI, F., AND TERZUOLO, C. A. Coordination of arm movement in three-dimensional space. Sensorimotor mapping during drawing movement. *Neuroscience* 17: 295–311, 1986.

SOECHTING, J. F. AND ROSS, B. Psychophysical determination of coordinate representation of human arm orientation. *Neuroscience* 13: 595–604, 1984.

SOECHTING, J. F. AND TERZUOLO, C. A. Organization of arm movements. Motion is segmented. *Neuroscience* 23: 39–51, 1987a.

SOECHTING, J. F. AND TERZUOLO, C. A. Organization of arm movements in three-dimensional space. Wrist motion is piece-wise planar. *Neuroscience* 23: 53–61, 1987b.

TAIRA, M., ASHE, J., SMYRNIS, N., AND GEORGOPOULOS, A. P. Motor cortical cell activity in a visually guided isometric force pulse task. *Soc. Neurosci. Abstr.* 17: 308, 1991.

THACH, W. T. Correlation of neural discharge with pattern and force of muscular activity, joint position, and direction of intended next movement in motor cortex and cerebellum. *J. Neurophysiol.* 41: 654–676, 1978.

VINCE, M. A. The intermittency of control movements and the psychological refractory period. *Br. J. Psychol.* 38: 149–157, 1948.

VIVIANI, P. AND STUCCHI, N. The effect of movement velocity on form perception: geometric illusions in dynamic displays. *Percept. Psychophys.* 46: 266–274, 1989.

VIVIANI, P. AND TERZUOLO, C. Trajectory determines movement dynamics. *Neuroscience* 7: 431–437, 1982.

WOOD, J. E., MEEK, S. G., AND JACOBSEN, S. C. Quantitation of human shoulder anatomy for prosthetic control, part II. *J. Biomech.* 22: 294–303, 1989.